Photochemistry and Photobiology, 2003, 77(6): 653–658

Relationship Between Collagen Autofluorescence of the Human Cervix and Menopausal Status

Erin M. Gill[1], Anais Malpica[2], Raphael E. Alford[3], Audrey R. Nath[4], Michele Follen[5,6], Rebecca R. Richards-Kortum[7], and Nirmala Ramanujam*[1]

[1]Department of Biomedical Engineering, University of Wisconsin, Madison, WI;
[2]Department of Pathology, M.D. Anderson Cancer Center, Houston, TX;
[3]Department of Biomedical Engineering, Duke University, Durham, NC;
[4]Department of Bioengineering, Rice University, Houston, TX;
[5]Department of Obstetrics, Gynecology and Reproductive Sciences, The University of Texas Health Science Center, Houston, TX;
[6]Department of Gynecologic Oncology, M.D. Anderson Cancer Center, Houston, TX and
[7]Department of Biomedical Engineering, The University of Texas, Austin, TX

Received 13 February 2003; accepted March 2003

ABSTRACT

The goal of this study was to evaluate the effect of different menopausal states (pre- and post-) on the endogenous fluorescence of normal cervical tissues. In particular, the average fluorescence as well as the interpatient and intrasample variability in the average fluorescence of the epithelium and stroma were evaluated as a function of pre- and postmenopausal states. High-resolution fluorescence images at excitation–emission wavelengths of 440, 520 nm and 365, 465 nm were obtained from epithelia and stroma of freeze-trapped cervical tissue blocks maintained at −196°C. The fluorescence images were recorded using a low temperature optical scanner. Fluorescence images from a normal sample population (n = 27) were quantitatively analyzed, and the average epithelial and stromal fluorescence intensities were obtained. Data grouped according to menopausal status (pre- *vs* post-) showed statistically significant differences ($P < 0.002$) in stromal fluorescence. In particular, the cervical stroma of postmenopausal women showed (1) significantly greater average fluorescence and (2) greater interpatient and intrasample variability in the fluorescence, relative to that of premenopausal women. These results provide evidence for changes in collagen cross-linking with menopause.

INTRODUCTION

It has been estimated that in the United States, 12 200 cases of invasive cervical cancer will be diagnosed and 4100 women will die from this disease in 2003 (1). Risk factors include human papilloma virus (HPV) infection, increasing age, no previous Papanicolaou (Pap) smear, multiple sexual partners or high-risk male partners, first intercourse at an early age, sexually transmitted diseases, smoking and using nonbarrier birth control methods (2). Because symptoms are present only in advanced stages, effective screening and diagnostic techniques are needed. Current screening and diagnostic methods for cervical cancer include the Pap smear and colposcopy. Although Pap smear screening and diagnostic colposcopy have dramatically reduced the number of cervical cancer deaths over the past 50 years, there is still a critical need for promising new technologies that can potentially improve the accuracy and efficacy of these screening and diagnostic programs.

Optical methods offer an alternative for early diagnosis of cervical cancer. Optical methods are noninvasive, fast and relatively inexpensive technologies. A promising optical diagnostic technique for cervical squamous intraepithelial lesions (SIL) under development is fluorescence spectroscopy. Fluorescence spectroscopy has been demonstrated to successfully detect cervical SIL in women undergoing colposcopy (3–10). In a recent study, fluorescence excitation–emission matrices were measured from 351 sites from the cervices of 146 patients undergoing colposcopy. The unbiased sensitivity and specificity for discriminating between squamous normal tissue and high-grade SIL were 71 and 77%, respectively, using fluorescence spectra at three excitation wavelengths, 330–340, 350–380 and 400–450 nm (10).

Fluorescence spectroscopy of cervical cell suspensions and tissue cultures has revealed excitation–emission maxima that are associated with the known endogenous fluorophores: tryptophan, reduced nicotinamide adenine dinucleotide (NADH), flavin adenine dinucleotide (FAD) and collagen (11). Fluorescence spectroscopy of human cervical tissue at these excitation–emission wavelengths can probe the concentration and distribution of these endogenous fluorophores *in vivo*. NADH and FAD are found in epithelial cells and are associated with cellular metabolism (12), and collagen is the structural component of the extracellular matrix (12). Differences in the fluorescence spectra of the neoplastic and nonneoplastic cervix have been attributed to NADH and collagen;

¶Posted on the website on 5 May 2003.
*To whom correspondence should be addressed at: Department of Biomedical Engineering, University of Wisconsin-Madison, 2144 Engineering Centers Building, 1550 Engineering Drive, Madison, WI 53706, USA. Fax: 608-265-9239; e-mail: nimmi@engr.wisc.edu
Abbreviations: CIN, cervical intraepithelial neoplasia; FAD, flavin adenine dinucleotide; H&E, hematoxylin and eosin; HRT, hormone replacement therapy; NADH, nicotinamide adenine dinucleotide; Pap, Papanicolaou; SIL, squamous intraepithelial lesion.
© 2003 American Society for Photobiology 0031-8655/03 $5.00+0.00

in particular, an increase in epithelial NADH fluorescence and a decrease in stromal collagen fluorescence have been noted in dysplastic cervical tissues (13).

It is important to note that the biochemistry and morphology of healthy cervical tissue are complex and may be influenced by multiple factors such as menstrual-cycle phase, menopausal status and pregnancy. Therefore, it is essential to understand the variability in normal cervical tissue fluorescence to properly interpret differences between neoplastic and nonneoplastic tissues.

The cervix is composed of a mixture of fibrous, muscular and elastic tissue and is lined by squamous and columnar epithelia. Hormone levels have a significant influence on the epithelial and stromal layers of the cervix. In general, estrogen stimulates epithelial proliferation, maturation and desquamation, whereas progesterone inhibits maturation. In postmenopausal women, the squamous epithelium is atrophic because of the ceasing of epithelial maturation (14). During pregnancy, elevated gestational hormones (estrogen, progesterone) stimulate the enlargement and softening of the cervix. The enlargement is caused by increased vascularity and edema in the stroma. Cervical softening is due to the rearrangement of collagen fibers and accumulation of extracellular ground substance within the stroma (15). The cervical softening, together with enlargement, facilitates dilation of the cervix during labor (14).

Brookner *et al*. (11) characterized the endogenous fluorophores within normal human cervical tissue and evaluated the changes in the endogenous cervical fluorescence with age and menopause. Using a novel technique, they prepared short-term ''live'' tissue cultures of normal cervical biopsies and imaged the endogenous fluorescence from the epithelial and stromal layers using epifluorescence microscopy at excitation wavelengths of 380 and 460 nm. NADH is fluorescent at 380 nm excitation, whereas FAD is fluorescent at 460 nm excitation. Collagen fluoresces at both excitation wavelengths. The fluorescence images were stratified into three statistically distinct age groups with average ages of 31, 38 and 49 years. The endogenous epithelial NADH and FAD fluorescence did not display statistically significant differences between the three age groups. However, an increase in the stromal collagen fluorescence was observed in the 38 and 49 year age groups relative to that in the 31 year age group, suggesting an increase in collagen cross-linking with age (16). Because there was a relative increase in the number of postmenopausal patients with age, these results indicate that there is an increase in stromal collagen fluorescence in postmenopausal women, relative to that in premenopausal women.

The goal of this study was to directly evaluate the effect of different menopausal states (pre- and post-) on the endogenous epithelial and stromal fluorescence of normal human cervical tissues. In particular, the average fluorescence as well as the interpatient and intrasample variability in the average fluorescence of the epithelium and stroma were evaluated as a function of pre- and postmenopausal states. The experimental protocol involved high-resolution fluorescence imaging of epithelial and stromal cross sections of freeze-trapped cervical tissue blocks using a low-temperature optical scanner. The samples evaluated in this study are inherently different from short-term tissue cultures. The previously used tissue culture systems do not preserve the intact vasculature of the tissue. The freeze-trapped tissue blocks preserve the intact vasculature and metabolic state of the sample. Furthermore, the metabolic state of the tissue slices can be affected by diffusion of ambient oxygen into the sample. Diffusion of oxygen into the freeze-trapped tissue block is significantly reduced at the liquid nitrogen temperatures at which the tissues are imaged. The excitation–emission wavelength pairs used in this study were 365 nm excitation and 465 nm emission and 440 nm excitation and 520 nm emission, which are similar to those used in the study by Brookner *et al*. (11).

The results of the current study indicate a significant relationship between stromal collagen fluorescence and menopausal status, and these results are consistent with previous findings by Brookner *et al*. (11). Specifically, the cervical stroma of postmenopausal women shows (1) significantly greater average fluorescence as well as (2) greater interpatient and intrasample variability in the fluorescence relative to that of premenopausal women. The postmenopausal women evaluated in this study were on average significantly older than the premenopausal patients, suggesting that an increase in stromal collagen fluorescence with age and menopause are clearly linked.

MATERIALS AND METHODS

Determination of menopausal status. The protocol for this study was reviewed and approved by the Institutional Review Boards of the University of Texas M.D. Anderson Cancer Center, and written consent was obtained from each patient who participated in the study. The chart of each patient who participated in the study was reviewed by a board-certified professor of obstetrics and gynecology (M.F.) and verified by two other observers: a certified advance nurse practitioner and research nurse. The age of menarche, regularity of menses, last two menstrual cycles, changes in menses, intermenstrual bleeding, symptoms of menopause, gravidity, parity, obstetrical history, contraceptive history, sexual history and history of treatment of dysplasia to the cervix were reviewed from all patient visits, including the study visit. The menopausal status was determined by the history of the last several menstrual cycles, the patient's age and the presence or absence of symptoms of menopause. Patients with menopausal symptoms were sent for follicle stimulating hormone (FSH) assays as part of the clinical protocol.

Sample collection. A normal-appearing and whenever possible an abnormal-appearing tissue sample were obtained per patient from a total of 21 patients who were undergoing colposcopy because of an abnormal Pap smear. Before sample collection, a small plastic container was filled with tissue-embedding medium (Tissue-Tek OCT, Sakura Finetek, Torrance, CA) and placed on a bed of ice. Each tissue sample was excised using a biopsy forceps and placed within the small plastic container. Each tissue sample was completely immersed and oriented such that the tissue surface was perpendicular to the surface of the embedding medium. Each tissue sample was then immediately transferred with the plastic container and rapidly frozen in liquid nitrogen to preserve the intact metabolic state and vasculature of the tissue for low-temperature fluorescence imaging (17). The average interval between excision and freezing was 1 min.

The cross section of the cervical tissue containing both the epithelium and stroma was exposed by shaving off layers of the embedding medium and tissue using a cryostat. Sectioning with the cryostat produced a flat cross section of the frozen cervical tissue block, which was necessary for subsequent fluorescence imaging. Before fluorescence imaging was carried out on the exposed surface of the frozen tissue block, a 5 μm thick section was cut and then stained with hematoxylin and eosin (H&E) for histological evaluation of the subsequently obtained fluorescence image.

Description of low-temperature fluorometer. A low-temperature fluorometer was used to obtain high-resolution fluorescence images from the exposed surfaces (of the epithelium and stroma) of frozen human cervical tissue blocks. A detailed description of the low-temperature fluorometer is provided elsewhere (18,19). In brief, the low-temperature fluorometer incorporates an optical scanner (mercury arc lamp, photo-multiplier tube, filters) with a stepper motor–driven light guide and a liquid nitrogen–filled sample compartment. The frozen tissue block is fixed in a chuck and then placed in the liquid nitrogen chamber. The tip of the light guide is submerged in the liquid nitrogen and then placed at a distance of 50 μm from an appropriate point on the tissue surface. During operation, the light guide is stepped across the tissue surface at a fixed increment, and fluorescence measurements are made from each discrete site. In this study,

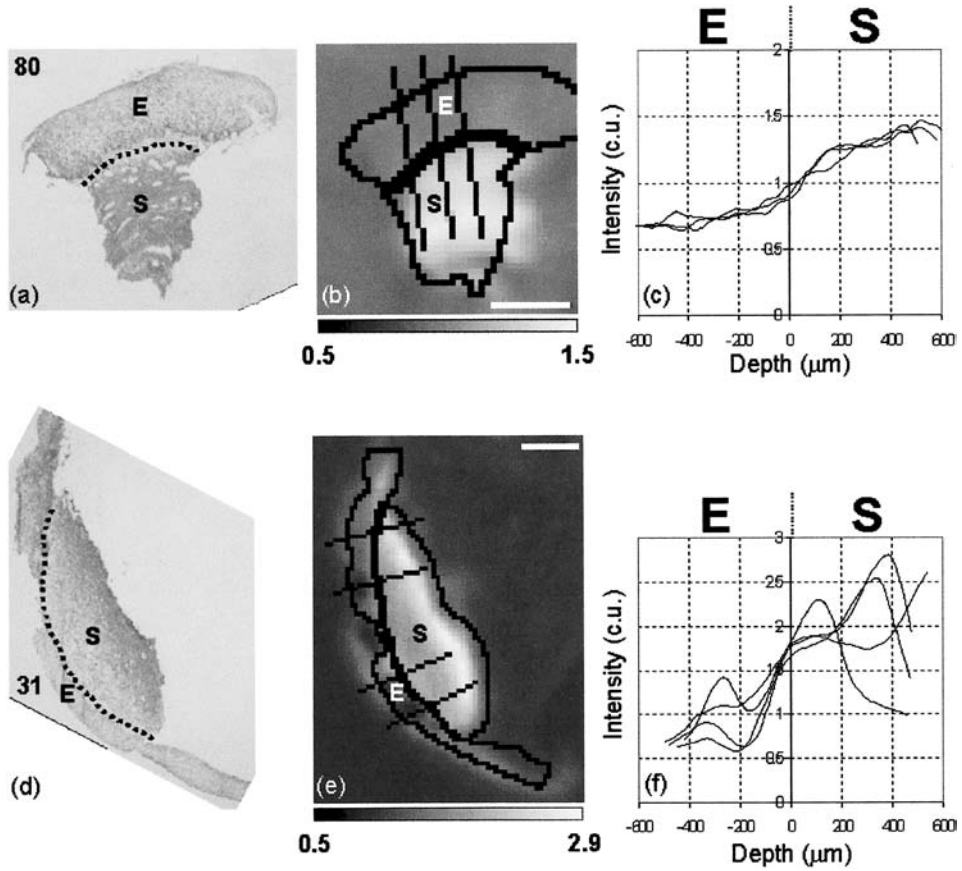

Figure 1. H&E-stained sections, fluorescence images at the excitation–emission wavelength pair of 440, 520 nm and corresponding fluorescence intensity depth profiles at 440, 520 nm, respectively, of two normal biopsy samples, samples 80 (a–c) and 31 (d–f). Sample 80 is from a 20 year old premenopausal patient, and sample 31 is from a 37 year old postmenopausal patient. The average epithelial thickness for sample 80 is 414 μm, and the average epithelial thickness for sample 31 is 194 μm. (a,d) indicate the location of the epithelium (E) and stroma (S). (b,e) indicate the fluorescence intensity distribution in the E and S regions and the line profile selections for the fluorescence intensity depth profiles in (c,f). The scale bars in (b,d) are 0.5 mm in length. (c,f) $E < 0$ and $S > 0$. Line profiles begin outside the fluorescence image and extend into the stroma.

the computer-controlled scan size was 128×128 pixels, the step size of the light guide was 40 μm, each pixel was sampled every 16 ms and four sampled points were averaged per pixel.

Fluorescence image acquisition. High-resolution fluorescence images were obtained from the frozen cervical tissue blocks at the following excitation–emission wavelength pairs: 365 nm excitation (25 nm band pass) and 465 nm emission (60 nm band pass) (365, 465 nm) and 440 nm excitation (20 nm band pass) and 520 nm emission (40 nm band pass) (440, 520 nm). The excitation filters were selected such that the center wavelengths of 365 and 440 nm coincide with the narrow lines of the mercury arc lamp at the same wavelengths. Thus, the excitation wavelengths are monochromatic and the excitation power is maximized. The two excitation–emission wavelength pairs selected for this study coincide with the excitation–emission maxima of NADH and FAD, respectively (11). These excitation–emission wavelength pairs are not optimal for collagen; however, they do yield detectable fluorescence from this strongly fluorescent molecule (11,13,20).

After each tissue experiment, fluorescence measurements were made from the surface of an absorption glass filter (OG 530, Omega) with the light guide at a fixed position and at a fixed distance (50 μm) from the surface of the filter using the identical experimental settings. The fluorescence intensity from each pixel on the tissue surface was divided by the fluorescence intensity from the standard to account for day-to-day variations in the source intensity and gain settings.

Histopathology. Each H&E–stained tissue section was evaluated by a board-certified pathologist (A.M.) and classified as normal squamous, normal columnar or cervical intraepithelial neoplasia (CIN).

Data analysis. Fluorescence images were analyzed using ''ImageJ'' imaging software. These images were coregistered with digital images of the H&E sections, and epithelial and stromal regions were identified (see Fig. 1). The scale of the digital H&E images was determined by comparing it with that obtained from a ruler at the same magnification. The scale of the fluorescence images was determined from the number of pixels (128×128) and the pixel size (40 μm). The size and orientation of the fluorescence and corresponding H&E images were matched. Then, the boundary of the H&E images and the interface between the epithelium and stroma were outlined, and the outline was transferred to the fluorescence image. The average and standard deviation of the fluorescence intensity were calculated for the epithelial and stromal regions of all cervical tissue samples. Wilcoxon rank sum tests (21) were used to determine whether there are statistically significant differences in the epithelial and stromal fluorescence of pre- and postmenopausal patients.

RESULTS

Low-temperature fluorescence imaging was carried out on 43 cervical tissue biopsies from 21 patients. Six samples were discarded from the analysis because of distortion of histological sections from freezing artifact or poor co-registration with the fluorescence images. Of the 37 remaining biopsy samples, 27 were classified as normal squamous and 10 were classified as abnormal (six had CIN and four had either inflammatory changes or koilocytosis). The 27 normal samples served as the focus of this

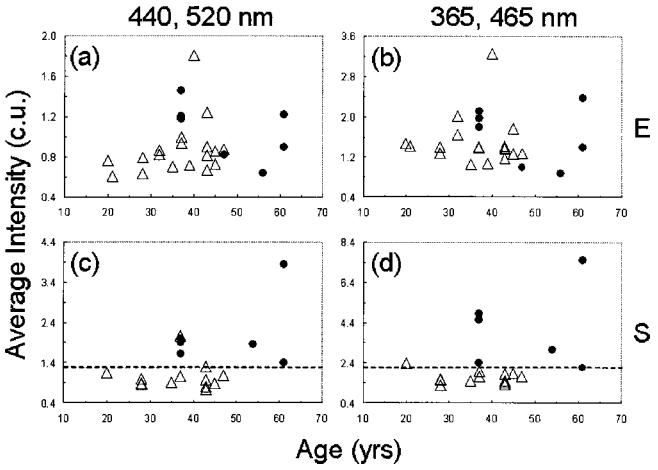

Figure 2. Average fluorescence intensity (averaged from all pixels within a sample region) *vs* age of the sample population at 440, 520 nm and 365, 465 nm, respectively: (a,b) for the epithelium (E) and (c,d) stroma (S). The open triangles are premenopausal, and black circles, postmenopausal. (a,b) include 25 total samples from 16 patients. (c,d) include 19 total samples from 12 patients. The dashed lines in (c,d) are included to aid visual discrimination.

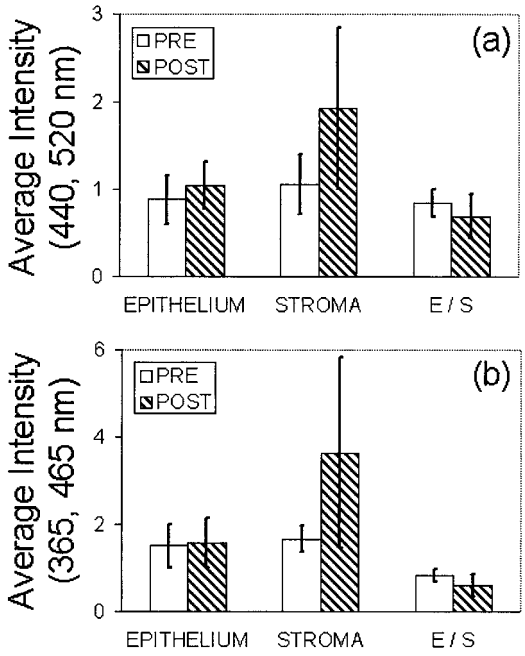

Figure 3. Average fluorescence intensities (averaged from all samples) of the epithelium and stroma and the average of the ratio of fluorescence in the epithelium and stroma (E/S) (a) at 440, 520 nm and (b) 365, 465 nm, grouped according to the patients' menopausal status (pre- *vs* post-). The samples from premenopausal patients include 12 samples with both epithelium and stroma, 6 samples with epithelium only and 1 sample with stroma only. The samples from postmenopausal patients include 5 samples with both epithelium and stroma, 2 samples with epithelium only and 1 sample with stroma only. The average stromal fluorescence intensities of postmenopausal patients are statistically greater than that of premenopausal patients ($P < 0.002$) at both excitation–emission wavelength pairs.

study. The patient population ranged in age from 20 to 61 years, with a mean age of 40 $\pm$ 11 years. Of the 27 samples, 19 were from premenopausal patients, and 8 were from postmenopausal patients. Three of the samples were from postmenopausal patients taking hormone replacement therapy (HRT) at the time of the study, and three of the samples were from postmenopausal patients who had undergone chemotherapy. Six of the samples were from premenopausal patients taking birth control pills at the time of the study. Twenty-four of the 27 samples were from patients with at least one earlier pregnancy.

Figure 1 displays H&E stained sections, fluorescence images at the excitation–emission wavelength pair of 440, 520 nm, and corresponding fluorescence intensity depth profiles at 440, 520 nm, respectively, of two normal biopsy samples, samples 80 (Fig. 1a–c) and 31 (Fig. 1d–f). Sample 80 is from a 20 year old, premenopausal patient, and sample 31 is from a 37 year old, postmenopausal patient. The average epithelial thickness for sample 80 is 414 μm, and the average epithelial thickness for sample 31 is 194 μm. Both fluorescence images reflect a trend of higher stromal (S) than epithelial (E) fluorescence at 440, 520 nm. The fluorescence image and corresponding depth profiles of sample 80, from a 20 year old, premenopausal patient, exhibit uniform fluorescence across the epithelium and the stroma. The fluorescence image and corresponding depth profiles of sample 31, from a 37 year old, postmenopausal patient, exhibit a higher degree of variability within the epithelium and stroma. These trends were similarly reflected in the fluorescence images at the excitation–emission wavelength pair of 365, 465 nm.

Figure 2 shows the average fluorescence intensity (averaged from all pixels within a sample region) *vs* age of the sample population at 440, 520 nm and 365, 465 nm, respectively, for the epithelium (Fig. 2a,b) and stroma (Fig. 2c,d). In this particular patient population, no clear trends with age are present at either of the excitation–emission wavelength pairs. However, when grouped according to menopausal status (as shown by the dashed line in Fig. 2c,d), the stromal fluorescence at both excitation–emission wavelength pairs of postmenopausal patients (black circles) shows higher average fluorescence intensities relative to that of premenopausal patients (open triangles).

Figure 3 shows the average fluorescence intensities (averaged from all samples) of the epithelium and stroma and the average of the ratio of fluorescence intensities in the epithelium and stroma (E:S) at 440, 520 nm (Fig. 3a) and 365, 465 nm (Fig. 3b), grouped according to the patients' menopausal status (pre- *vs* post-). The average stromal fluorescence intensities of postmenopausal patients are statistically greater than that of premenopausal patients ($P < 0.002$) at both excitation–emission wavelength pairs. The average epithelial fluorescence intensities and the average of the ratio of fluorescence intensities in the epithelium and stroma do not display statistically significant differences between premenopausal and postmenopausal patients.

Figure 4a,b shows two-dimensional scatter plots of (1) average fluorescence intensities (averaged from all pixels within a sample region) and (2) the corresponding standard deviation (σ) in the average fluorescence intensities at the excitation–emission wavelength pairs 365, 465 nm and 440, 520 nm of the stroma only ($n = 19$). The average stromal fluorescence intensities from premenopausal patients cluster together (open triangles) at the lower left-hand corner of the plot, whereas those from postmenopausal patients (black circles) increase at both excitation–emission wavelength pairs. The standard deviations of the average stromal fluorescence intensities exhibit similar trends.

DISCUSSION

In this study, fluorescence patterns of normal cervical tissue were characterized using low-temperature, high-resolution fluorescence imaging. The epithelial fluorescence is attributed to that from NADH at 365, 465 nm and that from FAD at 440, 520 nm (11). The stromal fluorescence at both excitation–emission wavelength pairs is attributed to collagen cross-links (11, 13). At both the excitation–emission wavelength pairs, 365, 465 nm and 440, 520 nm, the average stromal fluorescence intensity was greater than the average epithelial fluorescence intensity within a sample for the majority (15 out of 17) of samples from patients ranging in age from 20 to 61 years. These results suggest that collagen fluorescence in the stroma is stronger than NADH or FAD fluorescence in epithelial cells. Brookner *et al*. (11) also observed relatively higher fluorescence from collagen in the stroma relative to NADH and FAD fluorescence in the epithelium within a sample for samples collected from patients in the 38 and 49 year age groups. However, they observed the opposite trend within a sample for samples collected from patients in the 31 year age group.

A dramatic relationship was observed between stromal fluorescence and menopausal status. At both excitation–emission wavelength pairs, the stroma showed a significantly greater average fluorescence as well as greater interpatient and intrasample variability in fluorescence in postmenopausal women, relative to that in premenopausal women (Fig. 4). The single outlier in Fig. 4a corresponds to a sample from a premenopausal patient. At present, we cannot account for this outlier but it is interesting to note that a second normal biopsy included in our data set from the same patient was not an outlier.

The results shown in Fig. 4 suggest distinct physiological changes in the cervical stroma with menopausal status. Stromal collagen fluorescence is attributed to the cross-linking molecules, hydroxyl pyridinoline and lysyl pyridinoline (22), that connect single collagen fibers, thus providing rigidity to the cervical stroma (23). The connective tissue of the cervix has both great tensile strength and elasticity to perform the functions of maintaining pregnancy and dilation during labor and delivery. In a recent study (23), changes in cervical collagen fluorescence in guinea pigs were evaluated during gestation. Collagen fluorescence decreased with cervical softening during pregnancy and then gradually increased with a return to the rigid state of the cervix postpartum. There is also evidence that the amount of collagen cross-linking in connective tissue increases with age (16). Taken together, evidence for changes in stromal collagen fluorescence with gestation (23), age (16) and menopausal status (11) (present study) suggests a relationship between collagen fluorescence and hormonal regulation. It is possible that the decline in estrogen with menopause (as is also the case with postpartum women) leads to an increase in collagen cross-linking and thus increased stromal fluorescence. This hypothesis may be tested by monitoring changes in cervical tissue fluorescence with the introduction of exogenous estrogen, such as with HRT.

This study demonstrates that variability in normal cervical tissue fluorescence is significantly greater in postmenopausal women relative to that in premenopausal women. We therefore propose that the task of differentiating dysplasia from normal tissue will be less affected by interpatient and intrasample variability in premenopausal patients compared with that in postmenopausal patients. Moreover, the differences observed in collagen fluorescence with menopausal status suggest that this technique could be used to evaluate tissue states such as in term and preterm labor that are perturbed by variations in hormonal status (24).

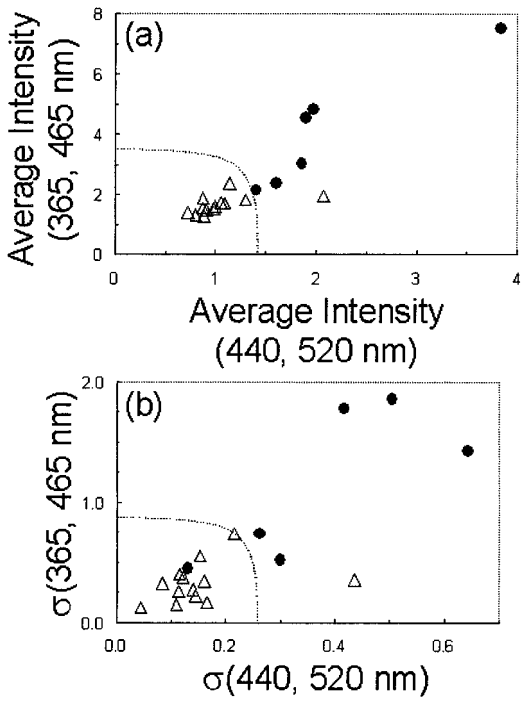

Figure 4. Two-dimensional scatter plots of (a) average fluorescence intensities (averaged from all pixels within a sample region) and (b) the corresponding standard deviation (σ) in the average fluorescence intensities at the excitation–emission wavelength pairs 365, 465 nm and 440, 520 nm of the stroma only (n = 19). The open triangles indicate premenopausal, and black circles indicate postmenopausal. The dashed lines are included to aid visual discrimination.

The results of this study have important implications with regard to fluorescence spectroscopy of human cervical tissues *in vivo*. In previous studies (3–10), fluorescence spectra have been measured from cervical tissues *in vivo* using fixed fiber-optic probe geometries; *i.e*. the illumination and collection areas are fixed. The measured fluorescence with these fiber-optic probes generally reflects the volume-averaged contributions from both the epithelial and stromal sublayers. Thus, the *in vivo* fluorescence spectra measured from the cervix will be influenced by (1) the intrinsic differences in the fluorescence of the epithelium and stroma and (2) the menopausal status–dependent intensity and variability of stromal fluorescence. The *in vivo* cervical tissue fluorescence spectra will also be influenced by the epithelial thickness and the optical properties of the epithelial and stromal layers, both of which will alter fluorescent light transport in the tissue.

These facts support the need for depth-resolved techniques that can locate the source of endogenous fluorescence within the different layers of cervical tissue. Fiber-optic probes for depth-resolved fluorescence spectroscopy have been recently proposed (25, 26). Alternatively, a model of light transport may be developed for resolving depthwise fluorescence from cervical tissues. Development of depth-resolved probes or mathematical models may overcome the above challenges and may ultimately aid in the interpretation of cervical tissue fluorescence spectra and the consequent diagnosis of tissue states that are hormonally or metabolically affected.

Acknowledgements—The authors gratefully acknowledge Professor Britton Chance, at the University of Pennsylvania, for providing access to the low-temperature fluorometer and for helpful discussions regarding the implications of this work. The authors would also like to acknowledge Christy Whitmore, Joanne Baker and Karen Rabel for assisting with collection of biographical data. This work was funded by the NCI (PO1 CA82710-01) and NIH 5 T32 GM08349.

REFERENCES

1. American Cancer Society, Inc., Atlanta, Ga. http://www.cancer.org/docroot/STT/stt_0.asp.
2. (2002) (NIH Publication No. 95-2047).
3. Weingandt, H., H. Stepp, R. Baumgartner, J. Diebold, W. Xiang and P. Hillemanns (2002) Autofluorescence spectroscopy for the diagnosis of cervical intraepithelial neoplasia. *Br. Obstet. Gynaecol.* **109**, 947–951.
4. Georgakoudi, I., E. E. Sheets, M. G. Muller, V. Backman, C. P. Crum, K. Badizadegan, R. R. Dasari and M. S. Feld (2002) Trimodal spectroscopy for the detection and characterization of cervical precancers *in vivo*. *Am. J. Obstet. Gynecol.* **186**, 374–382.
5. Georgakoudi, I., B. C. Jacobson, M. G. Muller, E. E. Sheets, K. Badizadegan, D. L. Carr-Locke, C. P. Crum, C. W. Boone, R. R. Dasari, J. Van Dam and M. S. Feld (2002) NAD(P)H and collagen as *in vivo* quantitative fluorescent biomarkers of epithelial precancerous changes. *Cancer Res.* **62**, 682–687.
6. Nordstrom, R. J., L. Burke, J. M. Niloff and J. F. Myrtle (2001) Identification of cervical intraepithelial neoplasia (CIN) using UV-excited fluorescence and diffuse-reflectance tissue spectroscopy. *Lasers Surg. Med.* **29**, 118–127.
7. Ramanujam, N. (2000) Fluorescence spectroscopy of neoplastic and non-neoplastic tissues. *Neoplasia* **2**, 89–117.
8. Wagnieres, G. A., W. M. Star and B. C. Wilson (1998) *In vivo* fluorescence spectroscopy and imaging for oncological applications. *Photochem. Photobiol.* **68**, 603–632.
9. Richards-Kortum, R. and E. Sevick-Muraca (1996) Quantitative optical spectroscopy for tissue diagnosis. *Annu. Rev. Phys. Chem.* **47**, 555–606.
10. Chang, S. K., M. Follen, A. Malpica, U. Utzinger, G. Staerkel, D. Cox, E. N. Atkinson, C. MacAulay and R. Richards-Kortum (2002) Optimal excitation wavelengths for discrimination of cervical neoplasia. *IEEE Trans. Biomed. Eng.* **49**, 1102–1111.
11. Brookner, C. K., M. Follen, I. Boiko, J. Galvan, S. Thomsen, A. Malpica, S. Suzuki, R. Lotan and R. Richards-Kortum (2000) Autofluorescence patterns in short-term cultures of normal cervical tissue. *Photochem. Photobiol.* **71**, 730–736.
12. Nelson, D. L. and M. M. Cox (2000) *Lehninger Principles of Biochemistry*. Worth Publishers, New York.
13. Drezek, R., C. Brookner, I. Pavlova, I. Boiko, A. Malpica, R. Lotan, M. Follen and R. Richards-Kortum (2001) Autofluorescence microscopy of fresh cervical-tissue sections reveals alterations in tissue biochemistry with dysplasia. *Photochem. Photobiol.* **73**, 636–641.
14. Wright, T. C. and A. Ferenczy (1994) Anatomy and histology of the cervix. In *Pathology of the Female Genital Tract*, (Edited by R. J. Kurman), pp. 142–157. Springer-Verlag, New York.
15. Leppert, P. C. (1995) Anatomy and physiology of cervical ripening. *Clin. Obstet. Gynecol.* **38**, 267–279.
16. Bailey, A. J. (2001) Molecular mechanisms of ageing in connective tissues. *Mech. Ageing Dev.* **122**, 735–755.
17. Chance, B., B. Schoener, R. Oshino, F. Itshak and Y. Nakase (1979) Oxidation-reduction ratio studies of mitochondria in freeze-trapped samples. NADH and flavoprotein fluorescence signals. *J. Biol. Chem.* **254**, 4764–4771.
18. Quistorff, B., J. C. Haselgrove and B. Chance (1985) High spatial resolution readout of 3-D metabolic organ structure: an automated, low-temperature redox ratio-scanning instrument. *Anal. Biochem.* **148**, 389–400.
19. Ramanujam, N., R. Richards Kortum, S. Thomsen, A. Mahadevan Jansen, M. Follen and B. Chance (2001) Low temperature fluorescence imaging of freeze-trapped human cervical tissues. *Opt. Express* **8**, 335–343.
20. Drezek, R., K. Sokolov, U. Utzinger, I. Boiko, A. Malpica, M. Follen and R. Richards-Kortum (2001) Understanding the contributions of NADH and collagen to cervical tissue fluorescence spectra: modeling, measurements, and implications. *J. Biomed. Opt.* **6**, 385–396.
21. Bethea, R. M., B. S. Duran and T. L. Boullion (1995) *Statistical Methods for Engineers and Scientists*. M. Dekker, New York.
22. Fujimoto, D., T. Moriguchi, T. Ishida and H. Hayashi (1978) The structure of pyridinoline, a collagen cross-link. *Biochem. Biophys. Res. Commun.* **84**, 52–57.
23. Fittkow, C. T., S. Q. Shi, E. Bytautiene, G. Olson, G. R. Saade and R. E. Garfield (2001) Changes in light-induced fluorescence of cervical collagen in guinea pigs during gestation and after sodium nitroprusside treatment. *J. Perinat. Med.* **29**, 535–543.
24. Garfield, R. E., H. Maul, W. Maner, C. Fittkow, G. Olson, L. Shi and G. R. Saade (2002) Uterine electromyography and light-induced fluorescence in the management of term and preterm labor. *J. Soc. Gynecol. Investig.* **9**, 265–275.
25. Quan, L. and N. Ramanujam (2002) Relationship between depth of a target in a turbid medium and fluorescence measured by a variable-aperture method. *Opt. Lett.* **27**, 104–106.
26. Zhu, C., Q. Liu and N. Ramanujam (2003) Effect of fiber optic probe geometry on depth resolved fluorescence measurements from epithelial tissues: a Monte Carlo simulation. *J. Biomed. Opt.* **8**, 237–247.